JOURNAL OF GEOPHYSICAL RESEARCH, VOL. 111, A11312, doi:10.1029/2006JA011855, 2006

Evidence for short spatial correlation lengths of the noontime equatorial electrojet inferred from a comparison of satellite and ground magnetic data

C. Manoj,[1] H. Lühr,[2] S. Maus,[3] and N. Nagarajan[1]

Received 15 May 2006; revised 14 August 2006; accepted 23 August 2006; published 9 November 2006.

[1] The current density of the noontime equatorial electrojet (EEJ) as determined from CHAMP data is highly variable between successive passes of the satellite, which are separated by 23° in distance and 93 min in time. An open question is to which extent this variability is caused by temporal or spatial variations in the ionosphere. Another important question is the connection between EEJ and global solar-quiet (S_q) current systems. We try to answer these questions by comparing the EEJ current density estimated from high-quality scalar magnetic field measurements of the CHAMP satellite with the magnetic horizontal intensity variations at six equatorial observatory pairs distributed across the globe. Data taken during the period 2000–2002 were used for the present study. We apply corrections for the effect of local time (LT) and S_q fields. By estimating the correlation coefficients between the ground and satellite data as a function of distances between measurements, new insights into the spatial structure of the EEJ have been obtained. The high correlation, when CHAMP passes directly over an observatory, decays quickly in eastern and western directions. Typically, within ±15° of longitudinal separation between satellite and observatory, the correlation falls well below the statistical significance level. This observation holds for all longitude sectors. Interestingly, the correlation between CHAMP-inferred EEJ strength and observatory differences breaks down for the observatory pairs, outside of a ±4° latitudinal band. This implies that the EEJ and S_q variations are uncorrelated for periods up to 1 hour. Additionally, it was found that monitoring of the EEJ can be performed best if the reference observatory is 4° to 5° apart from the dip equator.

Citation: Manoj, C., H. Lühr, S. Maus, and N. Nagarajan (2006), Evidence for short spatial correlation lengths of the noontime equatorial electrojet inferred from a comparison of satellite and ground magnetic data, *J. Geophys. Res.*, *111*, A11312, doi:10.1029/2006JA011855.

1. Introduction

[2] The equatorial electrojet (EEJ) is a narrow feature of intense electric current in the ionosphere which is confined to a latitude band of ±3° about the dip equator. Many studies have been devoted to the investigation of the EEJ with magnetometer array [*Rigoti et al.*, 1999; *Doumouya et al.*, 1998], rocket measurements [*Prakash et al.*, 1971], radar [*Crochet*, 1977], and satellite measurements [*Onwumechili and Agu*, 1980; *Langel et al.*, 1993; *Jadhav et al.*, 2002; *Lühr et al.*, 2004]. For more information on EEJ, see reviews by *Forbes* [1981], *Rastogi* [1989], and *Onwumechili* [1997]. Quite different aspects of the EEJ are highlighted by ground-based and satellite-based magnetic observations. While, from the ground, a continuous record of the current-induced magnetic field is obtained, polar orbiting satellites take just a snapshot of the latitudinal current distribution while passing over the equatorial region. Both data sets have their merits and limitations. The temporal variations recorded by a ground station do not offer any information on the spatial extent of the current system. Satellite measurements on the other hand give no information on the temporal variation of the EEJ due to the ambiguity between temporal and spatial structure. By combining both data sets, a complete spatiotemporal characterization of the EEJ can be obtained.

[3] So far, studies with simultaneous satellite and ground data have concentrated on local observations of the EEJ behavior. From these, it is not possible to derive the longitudinal structure of the current variations. One of the results derived from CHAMP satellite observations of the noontime EEJ is that the current density is highly variable. Crossings of the electrojet on successive orbits often revealed differences in the current density by a factor of 2 or more [*Lühr et al.*, 2004]. From orbit to orbit, the local time of the footprint stays virtually unchanged, but the satellite advances by about 23° westward in longitude.

[1] National Geophysical Research Institute, Hyderabad, India.
[2] GeoForschungsZentrum, Potsdam, Germany.
[3] CIRES, University of Colorado and NOAA's National Geophysical Data Center, Boulder, Colorado, USA.

0148-0227/06/2006JA011855$09.00

The open question is, What is the reason for the large changes in current strength? Is it the temporal variation within 93 min duration of the orbital period or the spatial variation over 23° in longitude?

[4] Another open issue, which has been pending for several decades, is the question about the connection between the EEJ and the S_q current systems [*Fambitakoye and Mayaud*, 1976]. While *Raghavarao and Anandarao* [1987], *Mann and Schlapp* [1988], and *Okeke et al.* [1998] argue that the S_q and EEJ current systems are independent, findings by *Schlapp* [1968], *Forbes* [1981], and *Hesse* [1982] support a coupling between the S_q and EEJ current systems. If these two current systems are closely coupled, they should show similar temporal variations.

[5] In this paper we try to provide answers to these questions. The approach is to combine measurements of the CHAMP satellite with data from ground-based magnetic observatories. For the retrieval of the EEJ signal from the ground magnetic field measurements, the difference is calculated between readings of a station close to the EEJ and another about 15° in latitude apart. We consider data from six station pairs, which are reasonably well distributed over the globe.

[6] The EEJ intensities derived from ground stations are compared with simultaneous current density estimates from close passes of the CHAMP satellite. These two independent estimates of EEJ strength are used in a correlation analysis to find out the spatial scale lengths over which the EEJ is coherent. The CHAMP data set considered here is for the years 2000 through 2003. The results thus reflect solar maximum conditions.

[7] In the following sections, we first describe the data processing of the satellite as well as ground data. Subsequently, we present the results of our correlation analysis for different sectors around the globe. Finally, we discuss the implications of the findings with reference to previous publications in this field.

1.1. Previous Studies on Longitudinal Extent of Equatorial Electrojet

[8] There are very few reported attempts to estimate the longitudinal extent of the noontime equatorial electrojet. POGO satellite data were used by many authors to study the EEJ as well as to obtain its correlation with ground data [*Yacob*, 1977; *Agu and Onwumechili*, 1981]. However, the studies were limited to finding the correlation coefficient and slope of the scatter for a large longitudinal window (20°, in most cases) above an observatory. The quality of data from POGO was not suitable to answer the questions we try to address here. MAGSAT crossed the EEJ only during dawn and dusk [*Langel et al.*, 1993]. Ørsted flies at an altitude of around 800 km and makes noontime crossings of the EEJ. *Jadhav et al.* [2002] calculated the cross-correlation matrix between the pairs of the daily estimates of EEJ strengths from the Ørsted data in 18 longitudinal bins each with 20° width. They find that the correlations of daily EEJ estimates are not systematic across the globe, with even the neighboring bins exhibiting poor correlation. Compared to Ørsted, CHAMP flies at lower altitude (~400 km) and has higher-resolution instrumentation, together making CHAMP more suitable to study the details of the EEJ.

[9] Occasionally, the normal eastward directed electrojet appears to reverse into a westward counter electrojet (CEJ). Counter electrojets are observed as depressions in the horizontal intensity in the diurnal variations measured in the equatorial regions and are assumed to be caused by a reversal of the EEJ current in the ionosphere. *Kane and Trivedi* [1981] and *Rangarajan and Rastogi* [1993] describe the morphology of CEJ as measured at observatories spaced ~35° apart. They find that CEJ events observed at one observatory are not always observed in the other observatories on the same day, concluding that the CEJ is a local phenomenon confined to within 35° longitude. However, they did not find any major difference in EEJ events between the observatories. Since CEJ events occur mostly in the morning and evening time and chances of their occurrence close to local noon time are rare [*Rastogi*, 1974, Figure 2], we do not expect any significant change in our correlative study due to CEJ. In addition, *Mann and Schlapp* [1988] did not find a significant influence of the CEJ on the correlation between the daily ranges of horizontal intensities between observatory pairs.

2. Observatory Data

[10] Geomagnetic hourly means of the horizontal intensities from 13 observatories were used in this study. Figure 1 shows the geographic distribution of the observatories. The observatories were grouped into six pairs, with one of the observatories in the immediate proximity to the dip equator (HUA, AAE, TIR, ETT, MBO, and GUA) and the other outside of the EEJ footprint area (FUQ, QSB, ABG, HYB, GUI, and CBI). The observatories within a pair have similar geomagnetic longitudes. The average latitudinal separation of the observatory pairs is 14.7°, with the HYB-ETT pair having the smallest separation of 8.42° and the QSB-AAE pair having the largest, with 24.85° (see Table 1). The longitudinal separation between observatory pairs is small, with a maximum of 4° for GUA-CBI. Whereas the Indian, African, and American sectors have reasonable numbers of observatory pairs, the Pacific region is only sparsely covered. An additional observatory (PND), in the Indian sector was used to verify the relation between EEJ and S_q fields.

[11] For most of the observatories, data were available up to December 2002. The data availability for each observatory in the time period 2000–2002 is shown in Figure 2. For the observatories TIR, AAE, and QSB, the available data were limited to 2 years. To limit the analysis to quiet days, both satellite and observatory data were screened for a magnetic activity index of $Kp \leq 2$. Roughly 53% of the total observatory data set was thus available for the study.

[12] Each observatory pair consists of one observatory close to the EEJ footprint and a second one outside of this area but both within the same longitude sector. The equatorial electrojet strength for an observatory pair is computed from the horizontal intensity, H, as $\Delta H_{EEJ} - \Delta H_{NonEEJ}$ [see, e.g., *Yacob*, 1977; *Alex and Mukherjee*, 2001; *Anderson et al.*, 2002], where ΔH is the variation of H from the mean midnight level for that observatory. Ideally, this differencing removes the core and large-scale magnetospheric fields from the data, and on magnetically quiet days ΔH describes the daily variation of S_q and EEJ plus their induced

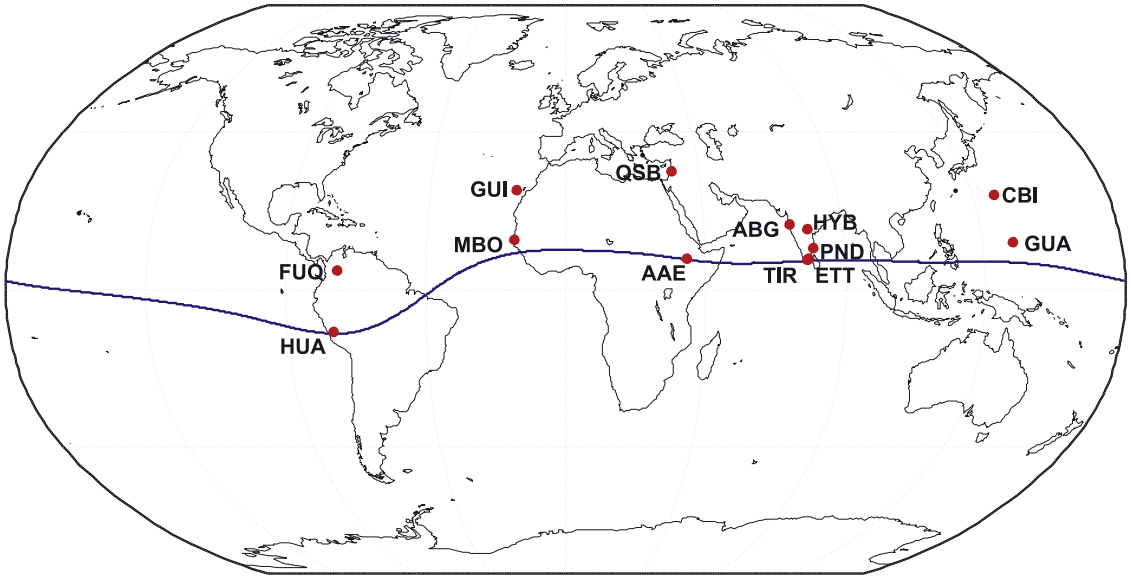

Figure 1. Distribution of the geomagnetic observatories used for the study. The blue line indicates the geomagnetic dip equator.

components. As an example, the average daily variation of the electrojet strength observed at ETT with respect to HYB for the period January 2000 to December 2002 is given in Figure 3. The EEJ strength reaches a maximum of 53 nT, just before noon at about 1100 LT. The rising flank of the EEJ signal in the morning hours (0700–1000 LT) is steeper than the afternoon decay (1300–1700 LT). Time series of hourly means of the EEJ strength were prepared for all the observatory pairs in a similar fashion.

3. Satellite Data

[13] We use the high-quality total intensity (scalar) magnetic field data measurements by the polar orbiting satellite CHAMP, for the time period 1 August 2000 though 1 April 2003 to determine the EEJ current distribution. Since the observatory data were limited to the period 2000 through 2002, the effective overlap period of the ground and satellite data sets is 1 August 2000 to 31 December 2002. We select for the analysis data from the local noon sector 10–13 hours, on magnetically quiet days (Kp $\leq$ 2). In total, 1653 crossings of the equator are considered. The measured magnetic field contains contributions from various sources. To study the signals related to the EEJ, all other contributions were removed carefully with the help of recent field models. For the geomagnetic main field, Pomme 1.4 [*Maus et al.*, 2005] was subtracted. The lithospheric/crustal field was removed by using MF2 [*Maus et al.*, 2002]. The diamagetic effect, caused by the ambient plasma [*Lühr et al.*, 2003], was also corrected for. Finally, the S_q variations and the remaining large-scale magnetospheric current effects were removed by fitting a degree-2 spherical harmonic polynomial. For a detailed description on the data processing, see *Lühr et al.* [2004]. The average magnetic signature of the EEJ, as described by *Lühr et al.* [2004], shows a negative deflection at the dip equator of about 20 nT, flanked on both sides by positive shoulders indicating return currents. The current density distribution of the EEJ was modelled by a series of EW oriented line currents, separated by 0.5° in latitude and located at an altitude of 108 km. The induction effect is modelled assuming a conductosphere below a depth of 200 km.

[14] The average current density profile obtained by inverting the CHAMP electrojet signature is given in

Table 1. Geographic and Geomagnetic Locations of the Observatories Used

	Station	Code	Geographic Latitude	Geographic Longitude	Geomagnetic Latitude	Geomagnetic Longitude	Dip Latitude
1	Alibag	ABG	18.63	72.87	10.03	145.97	13.67
2	Etaiyapuram	ETT	9	78	−0.04	149.99	1.40
3	Hyderabad	HYB	17.42	78.55	8.29	151.29	11.66
4	Tirunelveli	TIR	8.67	77.82	−0.55	149.6	0.36
5	Huancayo	HUA	−12.05	284.67	−1.61	356.32	0.59
6	Fuquene	FUQ	5.47	286.27	15.92	357.77	17.06
7	M'Bour	MBO	14.39	343.04	20.26	57.32	4.59
8	Guimar	GUI	28.32	343.56	33.91	60.49	23.04
9	Addis Ababa	AAE	9.02	38.77	5.27	111.57	0.95
10	Qsaybeh	QSB	33.87	35.64	30.23	113.37	30.89
11	Guam	GUA	13.58	144.87	5.1	215.43	6.19
12	Chichijima	CBI	27.1	142.18	18.28	211.39	20.79
13	Pondichery	PND	11.92	79.92	2.7	152.13	4.75

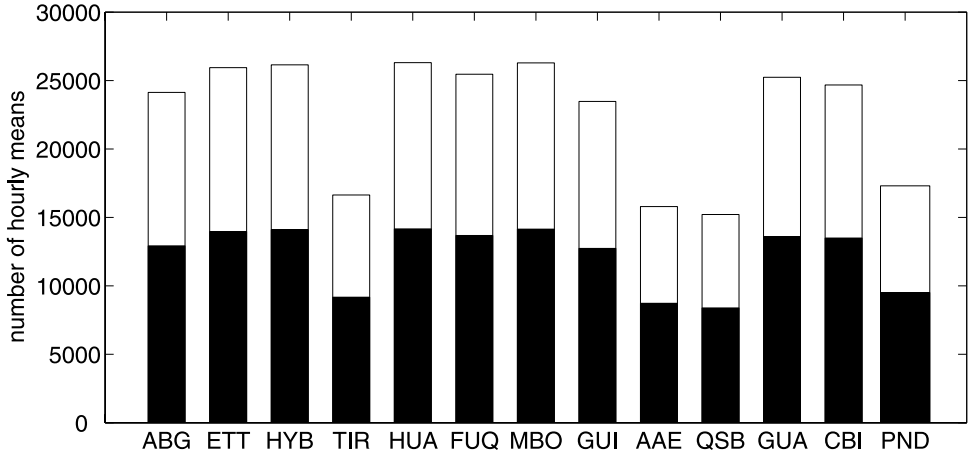

Figure 2. Availability of the hourly means from observatories. The white bars indicate the total available data sets and the dark bars indicate the subset for Kp $\leq$ 2.

Figure 4. It is clear from the figure that the current peak coincides with the dip equator and the return currents peak at ±5° from the dip equator. The total current was estimated by integrating the region of the EEJ separately for positive and negative current densities. Total average eastward current amounts to 65 kA and return current adds up to 21 kA. We use the peak-to-peak amplitudes of the current density profiles from the individual passes to correlate with the ground magnetic data. The peak-to-peak amplitude is defined as the average height of the positive peak with reference to the north and south troughs associated with the return currents (Figure 4). This we regard as a more reliable estimate than referring to the positive peak value, which is affected by uncertainties in the baseline of the presumed S_q signal.

[15] The predicted ground magnetic signature of the EEJ from the above (Figure 4) current density model gives quite interesting results. The latitudinal profiles for the field components, B_x, B_z, and the signature in total field, ΔB at ground are plotted in Figure 5. The total field deflection (ΔB) and the B_x (northward) component have almost identical magnitude and shape. This is due to the fact that EEJ currents are well confined to the region where the geomagnetic field lines are tangential to the Earth's surface. This also justifies scalar measurements to be used for characterizing the EEJ both in satellite and ground-based studies. On the ground, the magnetic signature due to return currents almost disappears. This is different for satellite data, which show prominent positive peaks for return current [*Lühr et al.*, 2004, Figure 3]. On average, the EEJ signal is visible on the ground only within a range of about ±4° latitude. This places stringent requirements on the location of ground observatories for EEJ monitoring. The locations of the observatories are plotted along the average profile, with respect to their distances from the dip equator. There is a certain dependence of the electrojet width on longitude, as shown by *Lühr et al.* [2004, Figure 6]. The half-peak width varies only within a range of less than 1°, attaining the largest width over South America and the smallest over East Africa. From these observations, we may deduce that the footprint latitudes for EEJ ground signatures are ±5° and ±4° for the two mentioned regions, respectively.

4. Data Processing

[16] The hourly estimates of the EEJ strength from different pairs of observatories distributed around the globe and the satellite derived EEJ current strength, as described in the earlier sections, form the data set for the correlation analysis. The data are further screened for magnetically quiet days with Kp $\leq$ 2 and for the time sector 1000–1300 LT, for both observatory and satellite data. By taking the data only between 1000 and 1300 LT, we limit our analysis to the period when the EEJ current is strongest, and we can ignore the morning and evening effects. For each observatory pair, the satellite data to be compared are binned according to their longitude of equator crossing with

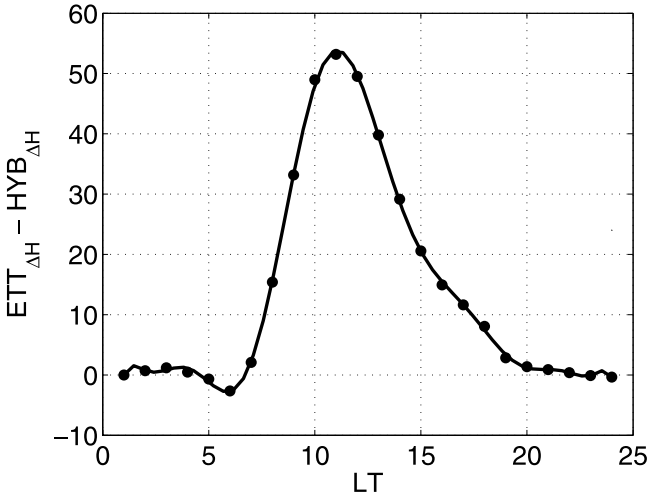

Figure 3. Average daily variation of the horizontal component of geomagnetic field observed at ETT with respect to the station HYB. ETT is close to the geomagnetic dip-equator and HYB is outside of the EEJ footprint area. The EEJ signal reaches a strength of 53 nT. The solid line represents a polynomial fit to the data.

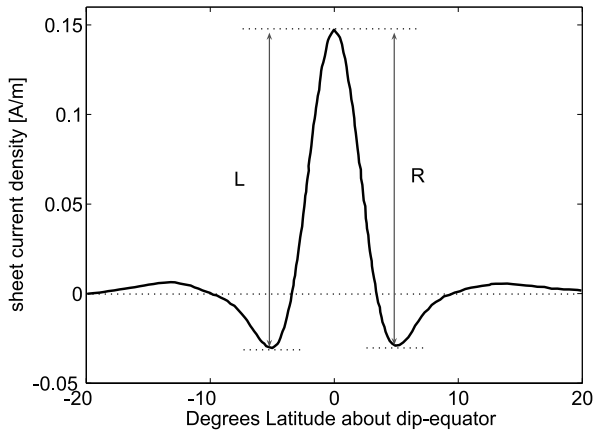

Figure 4. Average current density profile obtained by inverting the average electrojet signature measured by CHAMP (from *Lühr et al.* [2004]). Owing to an uncertainty in the baseline, the average height of the peak amplitude with reference to the left (L) and right (R) troughs was used for comparing with the ground magnetic data.

a bin size of 10°, centered on the longitude of the observatory pair. The choice of a bin size of 10° was a compromise due to the tradeoff between the number of required passes in each bin and the longitudinal resolution of the correlation analysis. For each bin the ground data and the corresponding satellite data are paired. Before we actually carry out the correlation, the observatory data had to be corrected for the local time effect as well as for S_q fields.

4.1. Local Time (LT) Correction

[17] Since the satellite crosses the dip equator at a certain LT and the corresponding observatory data may have a different LT, a correction has to be applied to make the data set comparable. Both data samples have to be normalized to the same local time. This is not very important for the satellite passes close to the observatory pair. However, as the satellite crosses the equator further away from the observatory location, the correction factor increases. For the correction procedure, we fit a degree-9 polynomial to the average daily EEJ variations for the observatory data (for example, Figure 3). For each satellite pass, the polynomial provides the corresponding amplitudes at the satellite and observatory local times. The ratio between these two numbers is used to normalize the actual observatory reading to the satellite local time. The effect of the correction, though small, is evident in the Figure 9. The LT correction increases the correlation coefficients.

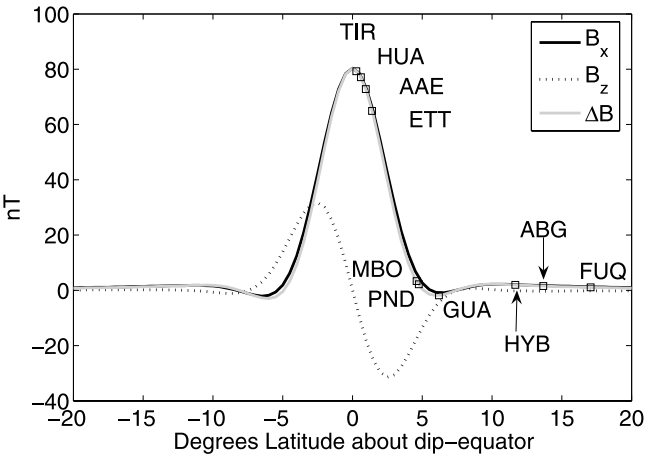

Figure 5. Predicted ground magnetic field profile due to the noon time equatorial electrojet from the CHAMP average current profile. The locations of geomagnetic observatories are plotted with respect to the dip equator along the magnetic field profile (Note that the vertical positions of the squares is not related to the measured data at observatories. Also, QSB and CBI are not shown here).

4.2. S_q Correction

[18] By subtracting the data from the nonequatorial observatory, we remove a major part of the S_q variation at the equatorial observatory. The unresolved part corresponds to the latitudinal difference of the S_q signal between the observatory pair, as illustrated in Figure 7. Toward lower latitudes, the S_q current becomes stronger. As an example, the daily variation of the difference between GUA-CBI is shown in Figure 6. Although neither of the two stations is directly below the EEJ, we obtain a daily variation of more than 50 nT. This S_q related signal would falsely be interpreted as part of the EEJ signal if were not removed from the difference of station pair. An ideal way to remove the S_q fields would be to have a dense latitudinal profile of geomagnetic stations across the dip equator [*Rigoti et al.*, 1999] enabling us to determine the EEJ and S_q currents separately. In the absence of that, we use the CM4 model [*Sabaka et al.*, 2004] to obtain an estimate of the latitudinal differences of the S_q signal between the observatory pairs. Latitudinal profiles of S_q fields were obtained for each pair by simulating the CM4 model with the actual solar flux, F10.7 as the controlling the parameter. The latitudinal profiles were thus computed for each of the observatory pairs and for each hourly average of the data interval. Figure 7 details an example from the ETT-HYB pair. A

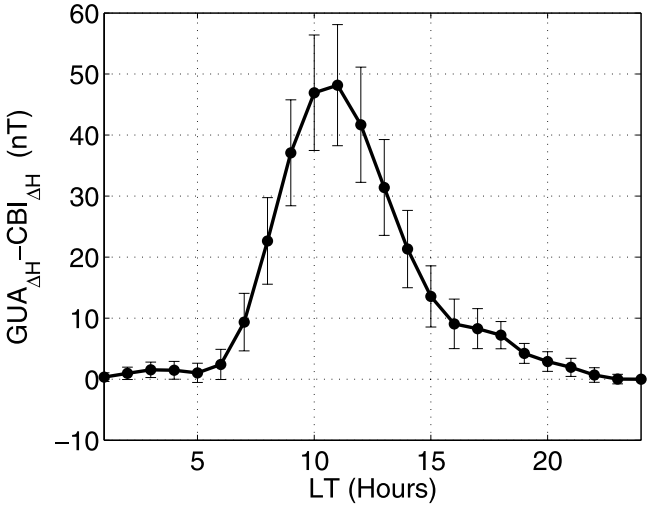

Figure 6. The average difference in daily variation between GUA and CBI. Although both observatories are away from the dip-equator, there exists a range of almost 50 nT. The error bars indicate the standard deviations.

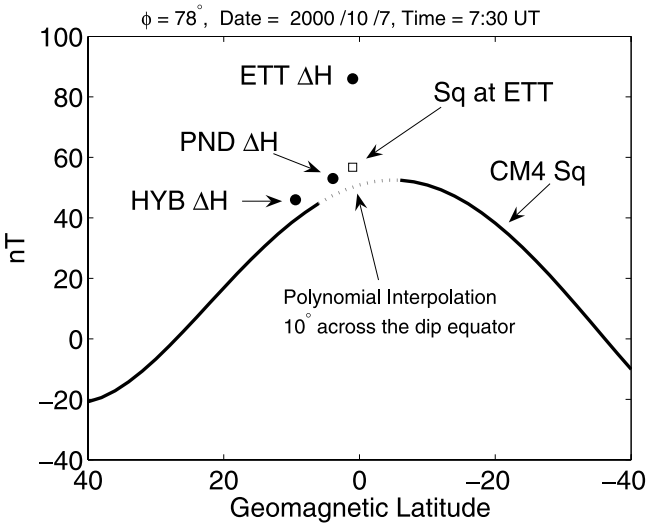

Figure 7. The latitudinal profile of the S_q field simulated from CM4 at the ground for the ETT-HYB pair (solid line). The black dots indicate the measured ΔH at HYB, PND and ETT. A degree-5 polynomial fit to the S_q profile is used to interpolate across EEJ latitudes. Using the slope of the S_q profile, and the ΔH reading at nonequatorial observatory, we estimate the S_q at the equatorial observatory. The open square indicates the estimated S_q amplitude at the equatorial station, ETT.

polynomial of degree 5 was fitted to each of these profiles. While fitting the CM4-derived S_q field, a region of 10° across the dip equator was deliberately masked to avoid an influence of the CM4 EEJ signature on the polynomial fit. The evaluation of the polynomial at the locations of the observatory pair gives the latitudinal difference of S_q field between them for each of the hourly means used. This latitudinal difference of the S_q fields was further subtracted to remove the unresolved part of the S_q variation at the equatorial observatory.

4.3. Effect of Time Lag Between Data Pairs

[19] CHAMP passes the equator at a certain UT, and it takes roughly 4 min to pass through the entire EEJ area. As hourly means of observatory data are compared with momentary satellite data, we verify the influence of the time difference between a satellite and observatory data pair. For the 0° longitude bin we looked for a relation between the residuals from the linear regression (see, for example, Figure 10) and the time difference of the two readings compared, after applying the LT correction. Figure 8 shows a scatterplot of the residual versus the time difference for ETT-HYB. No correlation between the two quantities is evident from the figure. The analysis was repeated for all the longitude bins and observatory pairs (not presented here). The result indicates that there is no systematic error/misfit produced by using hourly means.

5. Correlation Between Satellite and Ground Data

[20] The correlation coefficients between satellite and ground data are found for each bin, using a statistically robust procedure to ensure that few bad data points do not influence the final result. The correlation coefficients for the ETT-HYB observatory pair are plotted versus the longitudinal bins in Figure 9. The error bar is the inverse of the significance of the correlation. The significance level is computed by transforming the correlation to create a t-statistic having N-2 degrees of freedom, where N is the number of data pairs in a particular longitudinal bin. Except for the 30° separation bins, the significance of correlation is greater than 95%, implying that the estimation of the correlation coefficients is meaningful. The correlation coefficient in the central bin is 0.94 (significance $\sim$= 1.0) which is higher than the previous estimates for the Indian sector as 0.86 by *Jadhav et al.* [2002] who used Ørsted and 0.9 by *Yacob* [1977] who used POGO data for a similar analysis. *Agu and Onwumechili* [1981] also report a correlation of 0.8 from POGO over the Indian region. For most of these analysis, they used a single longitudinal bin of 20° width, namely, 60°–80°E over the Indian region. The improved correlation coefficient is to a good part due to the more precise data obtained from the CHAMP satellite. CHAMP flies lower above the ionosphere than the previous magnetic satellites, and the removal of magnetic fields from other sources is more sophisticated. However, other factors, like the width of the bin in time and space used for the correlation analysis might also have contributed to the reduction in correlation coefficients. A larger bin size reduces the correlation by averaging over the lower values of adjacent bins. The high correlation coefficient justifies the approach used here to compare the CHAMP-EEJ current density with the magnetic EEJ signal from the observatories.

[21] The most striking finding from the correlation analysis is the sharp decay of the correlation coefficients when the satellite passes at a further distance from the observatory longitude. This is evident from the near-symmetrical correlation plot (Figure 9). As we discuss in the later sections,

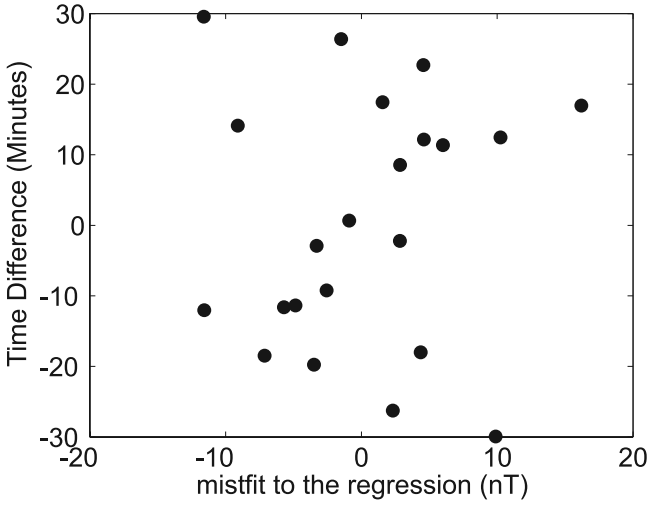

Figure 8. Plot of the misfit to the linear regression versus the time difference between the satellite crossing of the dip equator and the center of the hourly means for the ETT-HYB pair. The data are from the 0° bin, centered on the observatory pair. No systematic trend is evident.

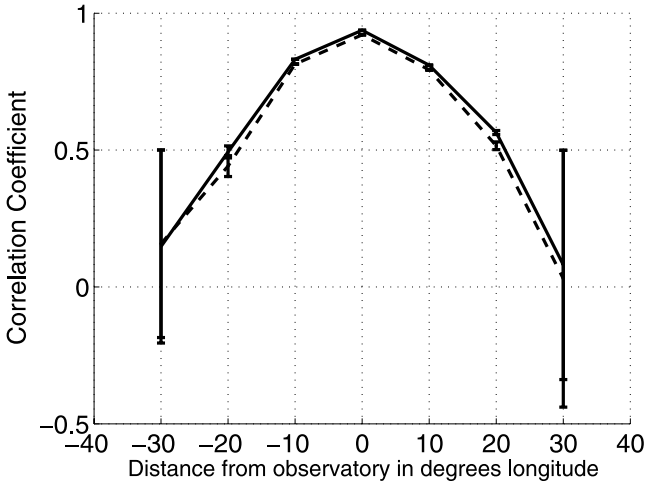

Figure 9. The correlation between the EEJ magnetic signals at ground and the satellite derived current density, plotted against the separation between the satellite and the equatorial observatory, here ETT (solid line). The dashed line indicates the same result, without LT correction.

this behavior is repeated over many sectors around the globe. Before getting into the interpretation of the small correlation length, we examine the scatter of the data in each bin, and the effect of the various corrections that we apply to the correlogram. Figure 10 represents essentially the scatter for each of the correlation coefficients plotted in Figure 9 for the ETT-HYB observatory pair. The remarkable linear relationship between the two data sets is evident in the 0° bin. However, as the distance gets longer, the scatter increases, and by the 20° bin, it deteriorates to a mere random scatter of data. The slope of a robust regression on the data from the 0° bin has a value 299.6 nT of ground magnetic signal to 1 A/m of the satellite inferred peak-to-peak current density.

[22] Correlation coefficients as a function of distance for each of the observatory pairs are shown in Figure 11. Plots are limited in longitudinal extent to ±40°, which is the maximum separation that can be handled with data limited to the LT sector 1000–1300 both for satellite and observatory. The observatory pairs from the Indian sector give the most symmetric correlograms. Here the S_q correction did not make any difference to the correlogram, indicating that by subtracting a non-EEJ station, we reasonably well accounted for the S_q field in the Indian sector. The ETT-HYB and TIR-ABG pairs give almost identical results. The estimation of the correlation coefficients are significant

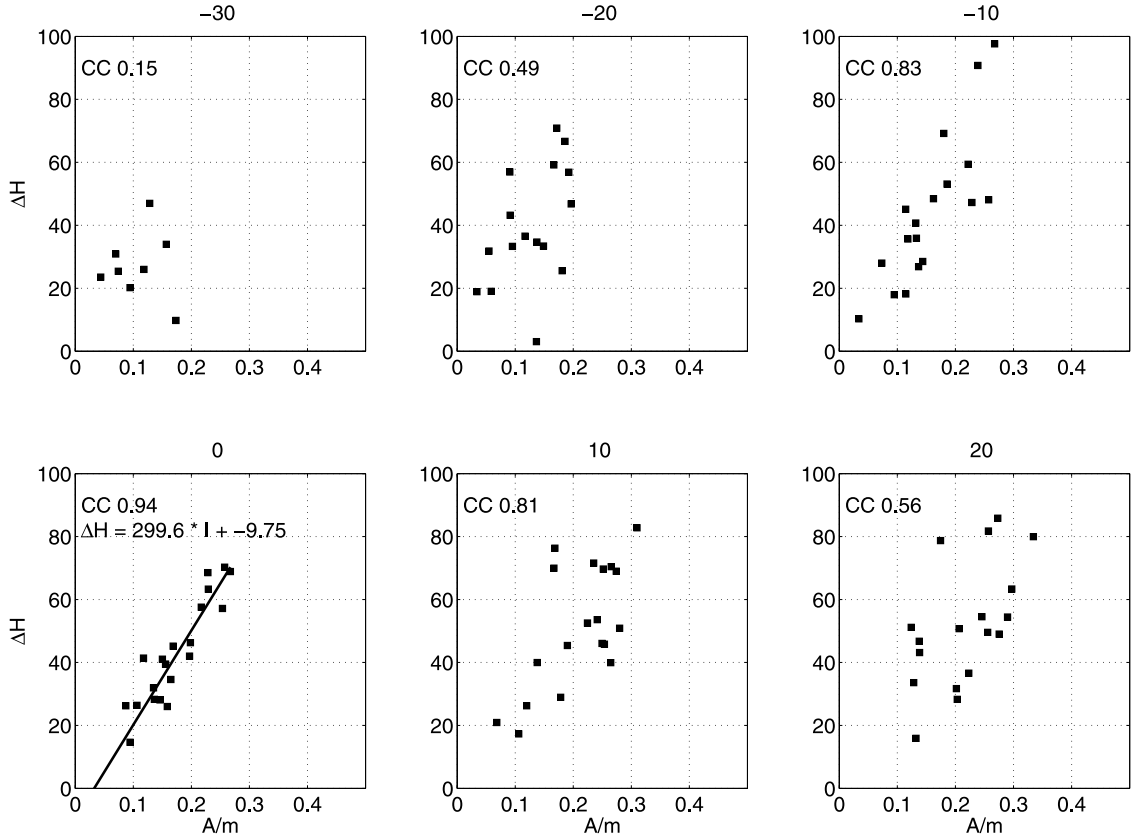

Figure 10. Plots of EEJ current density vs. ground magnetic strength for each longitudinal bin for ETT-HYB sector. The X axis represents the satellite inferred peak-to-peak current density and Y axis represents the EEJ magnetic signal strength observed by the observatory pair. The number on top of each panel shows the longitudinal distance in degrees from the observatory to the center of the satellite bin.

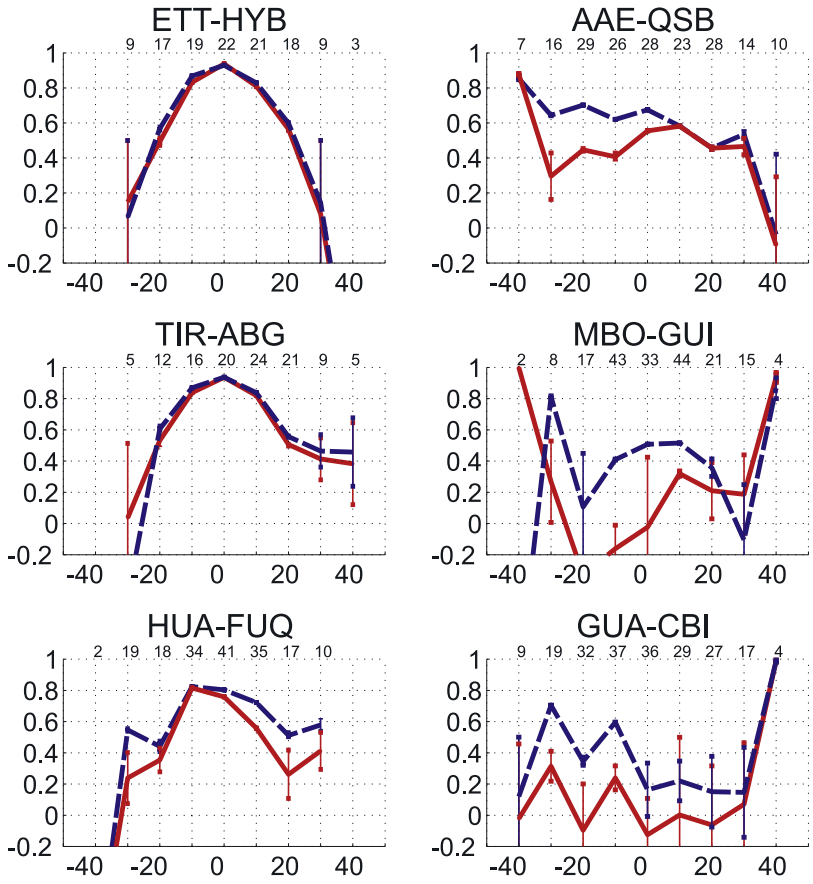

Figure 11. Correlation coefficients as function of distance from the observatories. The solid red line shows the correlation with S_q correction and the dashed blue line shows the correlation without S_q correction. The number of data points used to estimate the coefficients is indicated on the upper axis. The observatory pair used is indicated above each panel.

within ±30° on both sides. As expected, the central bin gives a high correlation between the satellite and ground data of 0.94. However, the value decays strongly, as the satellite passes further away from the station longitude. By following the statistical analogy that 0.7 is the limit of reasonable correlation between two data sets, we can assume a correlation length of about ±15° for the noontime EEJ in the Indian sector. This length is the same for both observatory pairs. TIR-ABG shows a different decay curve on the eastern side of the observatory, after 20°. As the significance of estimation of correlation coefficients is not very high at this spacing, we do not attempt to interpret this difference.

[23] For the South American sector (HUA-FUQ), we have similar results, with the rapid decay of the correlation on both sides of the central bin. Here the S_q correction resulted in reducing the correlation coefficients on both sides of the central bin. Unlike the Indian sectors, the significant extent of the correlation (0.7) is somewhat asymmetrical and has a range of ±10°, i.e., 5° less. We do not regard the shift of peak in correlation coefficient to 10° west of the central bin as significant.

[24] In contrast to the Indian and American sectors, the East African sector (AAE-QSB) gives somewhat different results. As AAE is close to the dip equator (dip latitude 0.95°), we expected a similarly clear longitude dependence for the correlation coefficients. Though the correlogram shows decrease in values on both sides, the correlation coefficients have considerably smaller amplitudes. The central bin, for example, has a correlation of only 0.55 after S_q correction. This is well below the statistical significance of correlated processes. The S_q correction reduced the coefficients to the west of the central longitude. There could be several reasons for the low value of the correlation over AAE. (1) AAE data were available only for two years starting from 2001. (2) The nonequatorial observatory, QSB, is separated by 24.85° in latitude from AAE, which is the largest separation among all of the pairs, and (3) the EEJ has minimum strength at this longitudinal sector [*Lühr et al.*, 2004]. Comparing POGO noontime data with AAE horizontal intensity, *Agu and Onwumechili* [1981] also reported a very low correlation (0.5) between satellite and ground data.

[25] Perhaps, the results from the West African sector (MBO-GUI) are most intriguing. MBO (dip latitude 4.59°) is at the fringes of the EEJ footprint area. However, with uncorrected observatory data, we still get a weak correlation with the satellite EEJ signatures, which decreases with distance from the observatory (Figure 11). This dependency completely vanishes once we apply the S_q correction (solid line). We get a similar result from the observatory pair PND-HYB, in the Indian sector (Figure 12). Both MBO and

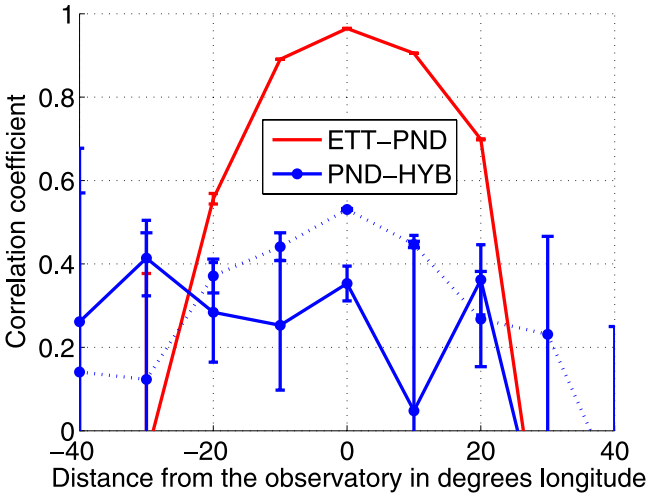

Figure 12. Plot of correlation between CHAMP current strength and ground magnetic data for two observatory pairs in the Indian sector. The ETT-PND pair (plotted with red line) has the highest correlation among all pairs used in the study. On the other hand, magnetic readings at PND, which is just 3° north of ETT, has no correlation with the satellite derived EEJ current density (plotted with solid blue line) when referenced with HYB. The weak dependency of the correlation values of this observatory pair (dotted blue line) disappears after the S_q correction. The PND is located at the fringes of EEJ and can act as a pivoting station to monitor both EEJ and S_q variations.

PND are located almost at the same distance from the dip equator (Figure 5). We will discuss this result in detail later. The last observatory pair shown here are GUA and CBI in Pacific Ocean. Unfortunately, both observatories are well outside the EEJ area (Figures 1 and 5). The correlation values do not show any dependency on the distance from observatory, with or without S_q correction. Here again, the S_q correction resulted in a clear reduction of the correlation coefficients.

[26] The obtained correlation coefficients for the 0° bin between the peak-to-peak current density estimated from CHAMP data and the EEJ signature on ground are summarized in Table 2. As mentioned before, the results from the Indian sector are quite outstanding. The quality of correlation seems to depend on the distance between the stations of a pair. More details on that are given in the next section. For stations outside of the EEJ footprint the S_q correction has a large effect. In the following section we will discuss possible explanations for the short correlation length of the EEJ and the relation between S_q and EEJ current systems.

6. Discussion and Conclusions

[27] In this study we have combined observations of the EEJ from ground and space to investigate the characteristics of this current system. A comparison of the EEJ peak-to-peak current density derived from above and the magnetic deflection observed from below reveals a linear relation of the quantities when the satellite passes directly over the ground station. For some station pairs in the Indian sector the correlation coefficient attains values beyond 0.9. This high degree of correlation supports our assumption that satellite and ground-based observations of the EEJ can be compared directly, when evaluated carefully.

[28] The main aim of this study is to find out the correlation length of the EEJ. For that reason we have also considered passes of the satellite further away from the ground station. At a longitudinal separation of 10°, the degree of correlation is still high, but at 20° it has already dropped below significance and for larger distances the observations are unrelated. This surprisingly short correlation length is in line with the results of the CHAMP statistical study of the EEJ [*Lühr et al.*, 2004]. From orbit to orbit the observed EEJ intensity was generally unrelated. From our ground/satellite comparison, performed at various longitude separations, we may conclude that this is primarily a spatial effect. Possible mechanisms responsible for the short correlation length will be discussed further down.

[29] Another topic we can comment on with our measurements is the relation between the S_q and EEJ current systems. Both are daytime phenomena exhibiting peak strength shortly before noon. When comparing the average daily variation of the differences between ETT-HYB (Figure 3), reflecting the daily range of the EEJ, and GUA-CBI (Figure 6), which we relate to the S_q variation, quite similar shapes are found. From this observation it became obvious that the differences between the station pairs should be corrected for the S_q effect before starting the correlation with the EEJ current density from satellite.

[30] Despite the excellent agreement in the average shape of the diurnal variation, there is no correlation found between the CHAMP EEJ estimates and the observations

Table 2. Correlation Between EEJ Peak-to-Peak Current Density and Magnetic Deflection on Ground, for the 0° Bin, Both With and Without S_q Correction

Station Pair	CC Without S_q Correction	CC With S_q Correction	Distance Between the Station Pair, deg	Distance of the Equatorial Observatory From Dip Equator, deg
ETT-HYB	0.93	0.94	10.26	1.40
TIR-ABG	0.94	0.94	13.4	0.36
HUA-FUQ	0.8	0.76	16.47	0.59
AAE-QSB	0.69	0.56	29.94	0.95
MBO-GUI	0.51	−0.02	18.45	4.59
GUA-CBI	0.163	−0.12	14.6	6.19
ETT-PND	0.97	0.97	3.35	1.40
PND-HYB	0.53	0.30	6.91	4.75

of GUA-CBI (cf. Figure 11 and Table 2). This is in contrast with the almost perfect correlation between CHAMP and ETT-HYB. From the location of the station pair GUA-CBI (cf. Figure 5) it becomes clear that it is outside the influence of the electrojet. We may thus conclude that the temporal variations of the EEJ and S_q current systems are decoupled for the spectral range considered here (about an hour). This is even more evident when looking at the correlation between CHAMP and the MBO-GUI pair. After correcting for the S_q effect, by means of CM4 model, no correlation is left (cf. Figure 11). With a distance of only 4.6° from the dip equator, MBO is just at the fringes of the EEJ footprint (cf. Figure 5). Already there, the EEJ current signatures derived from CHAMP are decoupled from the ground magnetic variations. This result suggests that the EEJ strength can be sensed (on the ground) only within a range of ±4° in latitude from the dip equator.

[31] For a further investigation of the relation between the EEJ and the S_q system, we have considered the data of an additional observatory in the Indian sector, PND, which is in between HYB and ETT (cf. Table 1). According to the predicted EEJ profile at the Earth surface, as derived from CHAMP observations, PND is located at the fringes of the magnetic signature (cf. Figure 5). This seems to be a good position for an EEJ reference station that does not require any S_q correction. We therefore performed an additional correlation between the pair ETT-PND and CHAMP recordings. The obtained correlation coefficient of 0.97 reflects an almost perfect agreement between ground and space-based observations when the satellite is passing overhead, as can be seen in Figure 12. This positive result confirms our suggestion for a favorable location of the reference station some 4° to 5° apart from the dip equator, depending slightly on longitude.

[32] *Anderson et al.* [2002] studied the relationship between the vertical $\mathbf{E} \times \mathbf{B}$ drift velocity in the ionospheric *F* region and the daytime strength of the EEJ in the South American longitude sector. They obtained the EEJ strengths from the magnetic horizontal intensity data at an equatorial observatory in Peru, with reference to another observatory located 6° north of the equatorial observatory. They obtained a correlation of 0.9 between ΔH from this pair of observatories and the $\mathbf{E} \times \mathbf{B}$ drift measured by the Jicamarca ISR. The result from our study, that the favorable location for the reference observatory is 4° to 5° apart from the dip equator could also have implication on monitoring the $\mathbf{E} \times \mathbf{B}$ drift from ground magnetic stations.

[33] The station PND can also be used to monitor the S_q variation by considering the difference PND-HYB. When correlating this time series, without applying S_q correction, with the CHAMP EEJ estimates (see Figure 12) we obtain a similar curve as in the case of MBO-GUI. It could be that the correlation results are affected by the very different character of the measurements, snapshot from space, hourly average from ground. To test this possibility, we have performed a correlation between identical types of data using readings of the station pairs ETT-PND (for EEJ) versus PND-HYB (for S_q). The analysis reveals a coefficient of 0.52, which is almost identical to the value derived from the CHAMP versus PND-HYB comparison (cf. Figure 12). The S_q correction based on CM4 resulted in the removal of the weak correlation between CHAMP EEJ signatures and the magnetic deflections from MBO-GUI and also PND-HYB pairs. The only time-dependent parameter used in CM4 for computing S_q is the EUV index, F10.7. The intensity of EUV, closely following the solar cycle and exhibiting a clear variation with the solar rotation period, is expected to influence the EEJ and S_q currents at the same time. The removal of this slowly varying EUV influence makes the EEJ and S_q variations virtually uncorrelated in the considered period range.

[34] What may be the reason for the unrelated variation of the two neighboring current systems? A possible cause for the latitudinally very confined variations of the EEJ can be the penetration electric field associated with DP2 fluctuations [e.g., *Kikuchi et al.*, 1996, 2000]. These electric fields, originating in the auroral regions cause variations with periods up to about an hour. The amplitude of the resultant magnetic signatures near the dip equator is sometimes 10 times larger than at stations outside the Cowling channel [see *Kikuchi et al.*, 1996, Figure 2]. The importance of the penetration electric field for low-latitude electrodynamics is only now fully realized. The S_q system, on the other hand, is driven primarily by tidal winds which do not show short-period variations. More dedicated observational campaigns are needed to better investigate the coupling efficiency of the two adjacent current systems over the whole spectrum. In particular, a dense latitudinal chain of magnetometers could be used to separate the generic variations of the EEJ from those of the S_q system. With the approach used here, the comparison between ground and satellite observations, only statistical results for a limited period range can be obtained.

[35] What could be the reason for the fact that the variations of the EEJ currents are only coherent over a longitude segment of about ±15° (±1 hour)? Above we had suggested the penetrating E-field as the driver for the short-period variations. These fields are known to have a larger longitudinal extent than 30° [*Kobea et al.*, 2000]. Current strengths are, however, determined by two factors, the product of the electric field and conductivity. Since we have excluded the electric field, the conductivity may be responsible for the short-range coherence of the EEJ. A promising candidate for local conductivity modulation is plasma instability within the Cowling channel. Two types of plasma instabilities can change the conductivity of the ionosphere and impede the flow of the electrojet current: (1) the modified two-stream and the (2) gradient drift instabilities [see *Fejer and Kelley*, 1980]. Plasma instabilities in the noontime ionosphere have been studied by rocket [*Prakash et al.*, 1971] and by extensive radar measurements [*Crochet*, 1977, 1979; *Hanuise and Crochet*, 1981]. *Prakash et al.* [1971] found that the amplitude of instabilities in the *E* region is well correlated with the EEJ current strength but not so well correlated with the drift velocities. In the region above 105 km, the plasma instabilities are found to be developed even when the drift velocities are as low as 70 m s^{-1}. This is also supported by radar measurements, wherein plasma instabilities are reported even in the absence of turbulence in the ionosphere [*Crochet*, 1981]. Though plasma instabilities in equatorial regions are frequently observed, their origin is still unclear. *Gagnepain et al.* [1976] consider the effect of longitudinal gradients of electric fields and currents in EEJ and find that reversals of currents and electric field directions are possible

Table 3. List of Observatories Used for the Study

Organization	Country	Stations
Instituto Geográfico Agust Codazzi	COLOMBIA	FUQ
Addis Ababa University	ETHIOPIA	AAE
Institut Français de Recherche Scientifique pour le Dèveloppement	FRANCE	MBO
Indian Institute of Geomagnetism	INDIA	ABG, PND, TIR
National Geophysical Research Institute	INDIA	ETT, HYB
Japan Meteorological Agency	JAPAN	CBI
National Centre for Geophysical Research	LEBANON	QSB
Instituto Geográfico Nacional	SPAIN	GUI
US Geological Survey	UNITED STATES	GUA
Instituto Geofisico del Peru	PERU	HUA

in case of longitudinal gradients, in contrast to infinite-line electrojet models. However, they did not consider the conductivity gradients in the ionosphere. Our finding that the short correlation length of EEJ is primarily due to spatial factors can be justified, if plasma instabilities cause local conductivity discontinuities in the noontime Cowling channel. Owing to current continuity these discontinuities can force an appreciable part of the current lines to close through the side lobes in smaller cells within the ionosphere, making the EEJ a patchwork of independent cells. For the verification of this suggestion a dedicated measurement campaign would be needed including radar, magnetometer, rocket, and satellite observations of the electrojet.

7. Summary

[36] In this paper we have presented a correlation analysis between ground and satellite signals related to EEJ using the observations made during the solar maximum years 2000 to 2002. For satellite and ground data, corrections were made to eliminate signals from sources other than the EEJ. The high-quality data from CHAMP provided an opportunity to estimate the longitudinal and latitudinal correlation lengths of EEJ with respect to ground observations, for the first time. The concurrent observations of the EEJ from ground and space reveal very consistent results when the satellite is passing over the station. The correlation coefficient between these two data sets drops considerably when measurements are compared from sites further apart than 15° in longitude. We suggest that local plasma instabilities in the Cowling channel are responsible for the short longitudinal correlation length of the EEJ. In latitude the magnetic signature of the EEJ are even more confined. At a distance of 4.5° from the EEJ axis, the observed variations with period up to about an hour are already decoupled from changes in the EEJ current intensity. We relate this to the very different sensitivity of the two current systems to the penetration electric field. However, to address the various aspects of coupling between EEJ and S_q properly, a dedicated array of magnetometers is needed.

[37] **Acknowledgments.** We would like to thank the institutions/organizations listed in the Table 3 for operating the geomagnetic observatories used in this study. The operational support of the CHAMP mission by the German Aerospace Center (DLR) and the financial support for the data processing by the Federal Ministry of Education and Research (BMBF) are gratefully acknowledged. Additionally, C. Manoj and N. Nagarajan thank V. P. Dimri, Director, National Geophysical Research Institute for support and permission to publish this work.

[38] Amitava Bhattacharjee thanks Scott England and R. Rajaram for their assistance in evaluating this paper.

References

Agu, C. E., and C. A. Onwumechili (1981), Comparison of the POGO and ground measurements of the magnetic field of the equatorial electrojet, *J. Atmos. Terr. Phys.*, *43*, 801–907.

Alex, S., and S. Mukherjee (2001), Local time dependence of the equatorial counter electrojet effect in a narrow longitudinal belt, *Earth Planets Space*, *53*, 1151–1161.

Anderson, D., A. Anghel, K. Yumoto, M. Ishitsuka, and E. Kudeki (2002), Estimating daytime vertical E × B drift velocities in the equatorial F-region using ground-based magnetometer observations, *Geophys. Res. Lett.*, *29*(12), 1596, doi:10.1029/2001GL014562.

Crochet, M. (1977), Radar studies of longitudinal differences in the equatorial electrojet - A review, *J. Atmos. Terr. Phys.*, *39*, 1103–1117.

Crochet, M. (1979), HF radar studies of two-stream instability during an equatorial counter-electrojet, *J. Geophys. Res.*, *84*, 5223–5233.

Crochet, M. (1981), Review of the equatorial electrojet instability in light of recent developments in HF radar measurements, *J. Atmos. Terr. Phys.*, *43*, 579–588.

Doumouya, V., J. Vassal, Y. Cohen, O. Fambitakoye, and M. Menvielle (1998), The equatorial electrojet: First results from magnetic measurement, *Ann. Geophys.*, *16*, 658–676.

Fambitakoye, O., and P. Mayaud (1976), Equtorial electrojet and regular daily variation SR; II, the center of the equatorial electrojet, *J. Atmos. Terr. Phys.*, *38*, 19–26.

Fejer, B. G., and M. C. Kelley (1980), Ionospheric irregularities, *Rev. Geophys.*, *18*, 401–454.

Forbes, J. M. (1981), The equatorial electrojet, *Rev. Geophys.*, *19*, 469–504.

Gagnepain, J., M. Crochet, and A. D. Richmond (1976), Theory of longitudinal gradients in the equatorial electrojet, *J. Atmos. Terr. Phys.*, *38*, 279–286.

Hanuise, C., and M. Crochet (1981), 550m wavelength plasma instabilities in the equatorial electrojet. I - Cross-field conditions. II - Two-stream conditions, *J. Geophys. Res.*, *86*, 3561–3572.

Hesse, D. (1982), An investigation of the electrojet by means of ground-based magnetic measurements in Brazil, *Ann. Geophys.*, *38*, 315.

Jadhav, G., M. Rajaram, and R. Rajaram (2002), A detailed study of equatorial electrojet phenomenon using Ørsted satellite observations, *J. Geophys. Res.*, *107*(8), 1175, doi:10.1029/2001JA000183.

Kane, R. P., and N. B. Trivedi (1981), Confinement of equatorial counter electrojet to restricted longitudes, *J. Geomagn. Geoelectr.*, *33*, 379–382.

Kikuchi, T., H. Lühr, T. Kitamura, O. Saka, and K. Schlegel (1996), Direct penetration of the polar electric field to the equator during a DP 2 event as detected by the auroral and equatorial magnetometer chains and the EISCAT radar, *J. Geophys. Res.*, *101*, 17,161–17,174.

Kikuchi, T., H. Lühr, K. Schlegel, H. Tachihara, M. Shinohara, and T.-I. Kitamura (2000), Penetration of auroral electric fields to the equator during a substorm, *J. Geophys. Res.*, *105*, 23,251–23,262.

Kobea, A. T., A. D. Richmond, B. A. Emery, C. Peymirat, H. Lühr, T. Moretto, M. Hairston, and C. Amory-Mazaudier (2000), Electrodynamic coupling of high and low latitudes: Observations on May 27, 1993, *J. Geophys. Res.*, *105*, 22,979–22,990.

Langel, R. A., M. Purucker, and M. Rajaram (1993), The equatorial electrojet and associated currents as seen in Magsat data, *J. Atmos. Terr. Phys.*, *55*, 1233–1269.

Lühr, H., M. Rother, S. Maus, W. Mai, and D. Cooke (2003), The diamagnetic effect of the equatorial Appleton anomaly: Its characteristics and

impact on geomagnetic field modeling, *Geophys. Res. Lett.*, *30*(17), 1906, doi:10.1029/2003GL017407.

Lühr, H., S. Maus, and M. Rother (2004), Noon-time equatorial electrojet: Its spatial features as determined by the CHAMP satellite, *J. Geophys. Res.*, *109*, A01306, doi:10.1029/2002JA009656.

Mann, R. J., and D. M. Schlapp (1988), The equatorial electrojet and day-to-day variability of Sq, *J. Atmos. Terr. Phys.*, *50*, 57–62.

Maus, S., M. Rother, R. Holme, H. Lühr, N. Olsen, and V. Haak (2002), First scalar magnetic anomaly map from CHAMP satellite data indicates weak lithospheric field, *Geophys. Res. Lett.*, *29*(14), 1702, doi:10.1029/2001GL013685.

Maus, S., H. Lühr, G. Balasis, M. Rother, and M. Mandea (2005), Introducing pomme, the potsdam magnetic model of the earth, in *Earth Observation with CHAMP, Results from Three Years in Space*, edited by C. Reigber et al., pp. 293–298, Springer, New York.

Okeke, F. N., C. A. Onwumechili, and A. B. Rabiu (1998), Day to day varaibility of geomagnetic hourly amplitudes in low latitude, *Geophys. J. Int.*, *134*, 484–500.

Onwumechili, C. A. (1997), *The Equatorial Electrojet*, Gordon and Breach, New York.

Onwumechili, C. A., and C. E. Agu (1980), General features of the magnetic field of the equatorial electrojet measured by the POGO satellites, *Planet Space Sci.*, *28*, 1125–1130.

Prakash, S., S. P. Gupta, B. H. Subbaraya, and C. L. Jain (1971), Equatorial electrojet-Electrostatic plasma instabilities, *Nature Phys. Sci.*, *233*, 56.

Raghavarao, R., and B. G. Anandarao (1987), Equatorial electrojet and counter electrojet, *Ind. J. Radio Space Phys.*, *16*, 54–75.

Rangarajan, G. K., and R. G. Rastogi (1993), Longitudinal difference in magnetic field variations associated with quiet day counter electrojet, *J. Geomagn. Geoelectr.*, *45*, 649–656.

Rastogi, R. G. (1974), Westward Equatorial Electrojet during daytime hours, *J. Geophys. Res.*, *79*, 1503–1512.

Rastogi, R. G. (1989), The equatorial electrojet, in *Geomagnetism*, vol. 3, edited by J. Jacobs, pp. 461–525, Elsevier, New York.

Rigoti, A., F. H. Chamalaun, N. B. Trivedi, and A. L. Padilha (1999), Characteristics of the Equatorial Electrojet determined from an array of magnetometers in N-NE Brazil, *Earth Planets Space*, *51*, 115–128.

Sabaka, T. J., N. Olsen, and M. E. Purucker (2004), Extending comprehensive models of the Earth's magnetic field with Ørsted and CHAMP data, *Geophys. J. Int.*, *159*, 521–547.

Schlapp, D. M. (1968), Worldwide morphology of day to day variability of Sq, *J. Atmos. Terr. Phys.*, *30*, 1761–1776.

Yacob, A. (1977), Internal induction by the equatorial electrojet in India examined with surface and satellite geomagnetic observations, *J. Atmos. Terr. Phys.*, *39*, 601–606.

H. Lühr, GeoForschungsZentrum-Potsdam, D-14473 Potsdam, Germany. (hluehr@gfz-potsdam.de)

C. Manoj and N. Nagarajan, National Geophysical Research Institute, Uppal Road, Hyderabad, India PIN 500 007. (manoj@ngri.res.in)

S. Maus, CIRES, University of Colorado, David Skaggs Research Center, NOAA/NGDC E/GC1, 325 Broadway, Boulder, CO 80305-3328, USA. (stefan.maus@noaa.gov)